An E-band Compact Frequency Division Duplex Radio Front-end Based on Gap Waveguide Technology

An E-band Compact Frequency Division Duplex Radio Front-end Based on Gap Waveguide Technology

Abbas Vosoogh[1], Milad Sharifi Sorkherizi[2], Vessen Vassilev[3], Ashraf Uz Zaman[1], Zhongxia Simon He[3], Jian Yang[1], Ahmed A. Kishk[2], and and Herbert Zirath[3]
[1]Department of Electrical Engineering, Chalmers University of Technology, Gothenburg, Sweden, abbas.vosoogh@chalmers.se
[2]Electrical and Computer Engineering Department, Concordia University, Montreal, Canada
[3]Department of Microtechnology and Nanoscience, Chalmers University of Technology, Gothenburg, Sweden

***Abstract*—A compact module consisting of a novel integration of an antenna, a diplexer, and millimeter-wave active circuits for low latency wireless backhaul links working at E-band is presented in this paper. The proposed radio front-end module is built by four distinct layers which are vertically stacked with no electrical contact requirement between them based on gap waveguide technology. A 16×16 corporate-fed slot array antenna is successfully integrated with a 5^{th} order diplexer, as well as a transmitter (Tx) and a receiver (Rx) monolithic microwave integrated circuits (MMICs) in one package with a novel architecture and a compact form. The integrated radio front-end is able to simultaneously send and receive data by using a frequency division duplex (FDD) transmission scheme at 71-76 GHz and 81-86 GHz bands. A wireless data transmission is successfully demonstrated showing a data rate of 6 Gbit/s using 64 quadrature amplitude modulated (QAM) signal with a spectral efficiency of 4.4 bit/s/Hz. The proposed radio front-end provides the advantages of low loss, high efficiency, compact integration, and a simple mechanical assembly, which makes it a suitable solution for small cell backhaul links.**

***Index Terms*—Electromagnetic band gap (EBG), integration, frequency division duplex (FDD), millimeter-wave, gap waveguide, slot array antenna**

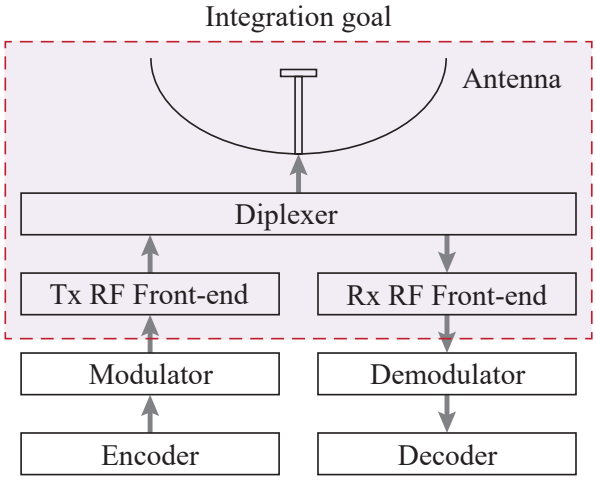

Fig. 1. Block diagram of a wireless Frequency division duplex (FDD) communication system.

I. Introduction

The use of the millimeter-wave frequency band (30-300 GHz) has been growing over the last few years in order to provide wider bandwidth and deliver more data rate [1]. Wireless backhaul link solutions with ultra-high data rate are desired as a flexible and cost-effective alternative to fiber optic networks to provide multi Gbit/s speed for the future wireless network systems. High path loss, atmospheric attenuation, and high sensitivity to weather conditions are some of the drawbacks of using millimeter-wave frequency bands [1]. However, the frequency range between 71 to 86 GHz (E-band) shows a low atmospheric attenuation of around 0.4 dB/km [1], which makes this frequency range a potential candidate to provide multi-Gbit/s data transmission.

Hollow waveguides show lower insertion loss compared to planar transmission lines such as microstrip lines and substrate integrated waveguides (SIW). Therefore, the metallic waveguides are suitable solutions for designing efficient and high performance RF components and systems. A plated-laminated waveguide filter and the integration with a 16×16 corporate-fed slot array antenna by diffusion bonding of several thin metal plates operating at E-band is presented in [2]. A combination of bandpass and bandstop filters is used to achieve a passband in 71-76 GHz and 81-86 GHz and reject the frequency band of 76-81 GHz. In [3] the integration of a high gain antenna with a diplexer with two channels at 71-76 GHz and 81-86 GHz is proposed based on gap waveguide technology. Gap waveguide technology is a low loss guiding structure showing the advantages of flexible manufacturing and mechanical assembly [4], [5]. In this new type of transmission line, there is no need for good electrical contact among the building blocks and any possible field leakage is avoided by using a stopband produced by an electromagnetic bandgap (EBG) structure [6].

In wireless backhaul links, it is important to send and receive data at the same time and maintain the data trans-

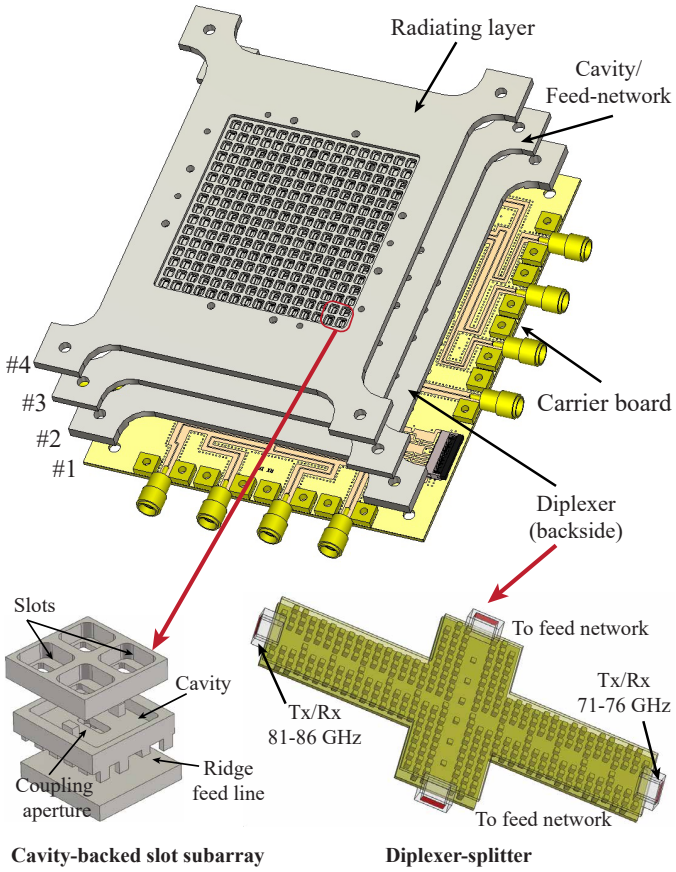

Fig. 2. Configuration of the proposed compact full duplex radio front-end.

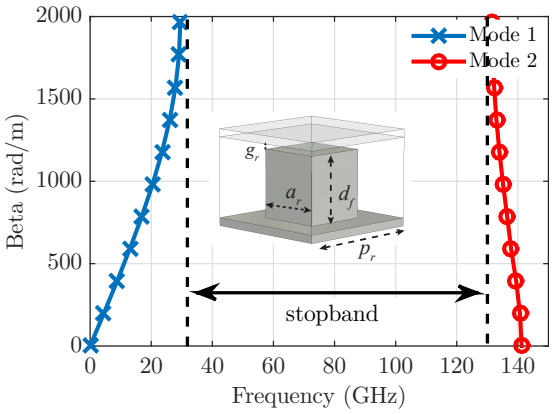

Fig. 3. Dispersion diagram of the infinite periodic pin unit cell (d_f = 0.7 mm, a_r = 0.64 mm, g_r = 0.04 mm, and p_r = 1.32 mm).

mission in both directions. Frequency division duplex (FDD) and time division duplex (TDD) are the two most widely used duplex schemes. The block diagram of an FDD wireless communication systems is shown in Fig. 1. In FDD systems, the transmitter and receiver operate simultaneously at different carrier frequencies to avoid interferences. The Tx and Rx chains are connected to one antenna via a diplexer. The diplexer provides two separate frequency channels with low interference to simultaneously transmit and receive data. At high frequencies, an FDD system usually consists of several bulky passive components, such as antennas and diplexers, which are separately assembled and packaged with high-frequency circuitries containing transceivers using several waveguide flanges. The goal of this paper is to show a compact integration of the Tx/Rx RF front-ends with the diplexer and a high gain antenna working at E-band, as it is illustrated in Fig. 1. In order to achieve the mentioned goal, we propose a full duplex radio front-end module suitable for multi-Gbit/s point-to-point wireless link applications based on gap waveguide technology.

II. Full Duplex Radio Front-end Configuration

Fig. 2 shows the configuration of the proposed solution. The integrated full duplex radio front-end module contains four distinct layers, i.e., Tx and Rx MMICs on a carrier board, a 5^{th} order diplexer, a corporate feed network, and 16×16 radiating slots. The layers are vertically stacked up, and each layer has a different functionality. The total size of the proposed module after assembly is 110 mm (length)×90 mm (width)×8.5 mm (thickness). A complete transmitter (Tx) and a receiver (Rx) GaAs chipsets are mounted and wire bonded to a carrier board at the bottom layer (layer 1). The carrier board consists of 100 μm Liquid Crystal Polymer (LCP) substrate, composed of a 50 μm Rogers Ultralam 3850HT which is bonded to a 1 mm copper plate with a 50 μm Rogers Ultralam 3908 bonding film. Coaxial interfaces provide LO inputs (11.8-14.3 GHz) and differential IF (0-12 GHz) inputs/outputs for the Tx and Rx.

Layer 2 contains a hybrid diplexer-splitter with two 5^{th} order bandpass filters. The RF signals from the Tx/Rx MMICs on layer 1 couple to the diplexer on layer 2 using a transition. The geometry of the designed diplexer-splitter is also shown in Fig. 2. The proposed diplexer is based on groove gap waveguide. The cavity resonators are formed by making a volume surrounded by pins. By moving the pins closer or away to the center of the cavity, the resonant frequency of the cavity can be controlled.

The radiating part (layers 3 and 4) of the proposed module is composed of 8×8 subarrays, where each subarray consists of 2×2 cavity-backed slots. Each four slots on layer 4 are fed by a cavity placed on topside of layer 3. The cavity is fed by a ridge gap waveguide line via a coupling aperture. Several gap waveguide based slot array antennas operating in different frequency bands and providing different gains have been previously reported [7]–[12], using similar radiating elements. A corporate feed network based on ridge gap waveguide is designed on the backside of layer 3.

The proposed integrated radio front-end has a simple mechanical assembly. There is no need for galvanic and electrical contact between the layers. The latter is due to the stopband that the EBG pin texture produces in gap waveguide technology. Fig. 3 shows the resulting dispersion diagram of a pin unit cell providing a stopband where there is the cutoff for all parallel plate modes. The Eigenmode solver of

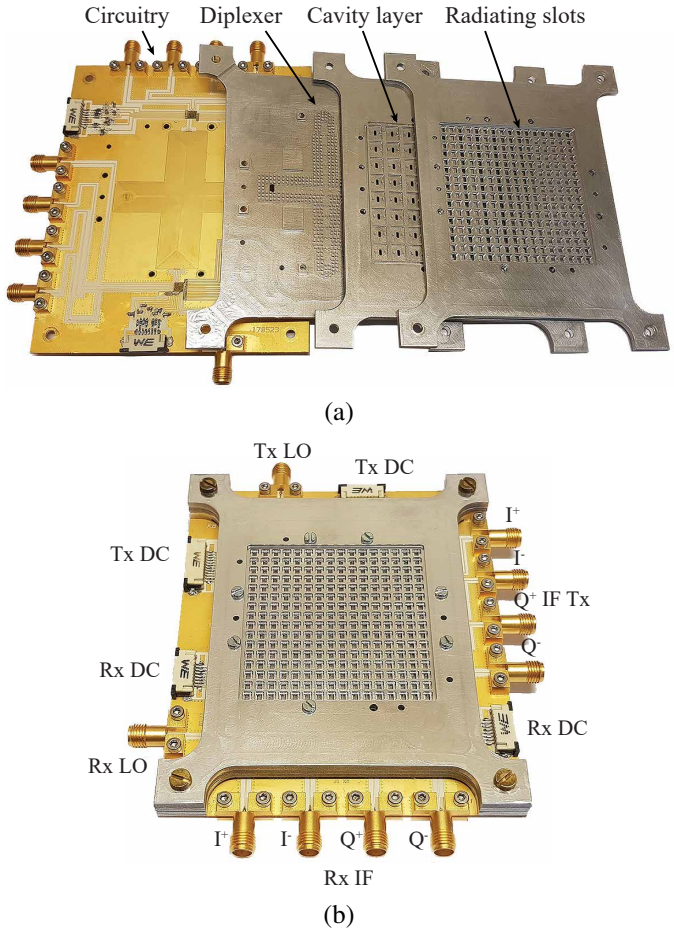

Fig. 4. Photograph of the fabricated prototype. (a) Different layers. (b) The full duplex radio front-end after assembly.

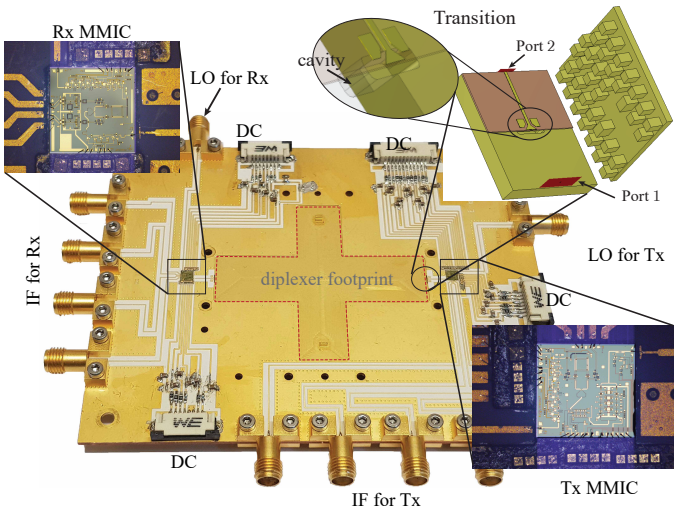

Fig. 5. Configuration of the designed carrier board.

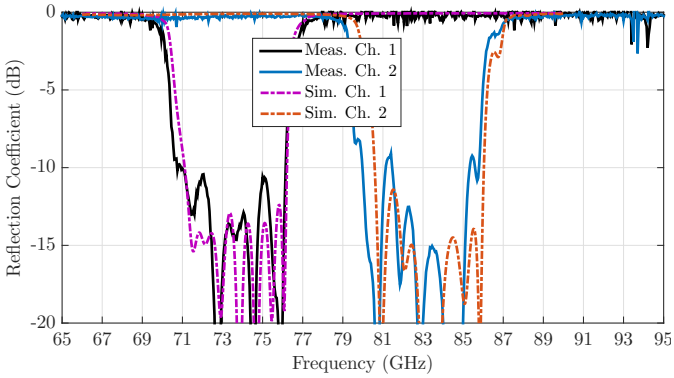

Fig. 6. Measured and simulated performance input matching of the integrated antenna-diplexer.

CST Microwave Studio is used to calculate such a dispersion diagram in the infinite periodic environment. The chosen pin unit cell with the given dimensions provides a stopband that covers sufficiently the whole frequency band of interest (E-band).

Fig. 4 shows the fabricated prototype, where we can differentiate all the layers of the module. The metal layers, i.e., the diplexer, the cavity, and the radiating layers, are manufactured by using CNC milling on aluminum. The printed circuit board (PCB) contains the millimeter-wave active circuitry, and it is illustrated in Fig. 5. We have used a commercially available complete Tx MMIC (part No. gTSC0023) covering the 71-86 GHz frequency band, and receiver MMICs for the 71-76 GHz (part No. gRSC0012) and 81-86 GHz (part NO. gRSC0013) frequency bands from Gotmic AB [13]. The MMICs are wire bonded to microstrip lines, as shown in Fig. 5. The carrier board supplies the required DC bias voltages of the Tx/Rx MMICs and coaxial interfaces for LO and IF ports. We have designed a compact contact-less transition from the microstrip line to groove gap waveguide as a low loss interface between the planar transmission line technology (microstrip line) and groove gap waveguide technology. As shown in Fig. 5, some parts of the LCP dielectric are removed at the middle of the carrier board, corresponding to the footprint of the diplexer.

We have fabricated and experimentally evaluated the performance of the different building blocks, i.e., array antenna, diplexer, packaged Tx/Rx, and transition. The measured and simulated reflection coefficients of the integrated antenna-diplexer, which has been fabricated separately, are shown Fig. 6. The simulated and measured results are in a good agreement, despite of a discrepancy in the measured results for the upper channel at 81-86 GHz band. This could be due to assembly errors and fabrication tolerances. Moreover, the far-field radiation pattern of the integrated antenna-diplexer in E- and H-planes at 86 GHz is illustrated in Fig. 6. Table I presents a summary of the measured performance of the different fabricated building blocks of the radio front-end module.

III. Wireless Link Demonstration

The designed module can be applied in a full-duplex FDD wireless communication scheme to operate in the 71-76 GHz and 81-86 GHz bands. Two modules have been used to demonstrate a wireless data transmission at E-band.

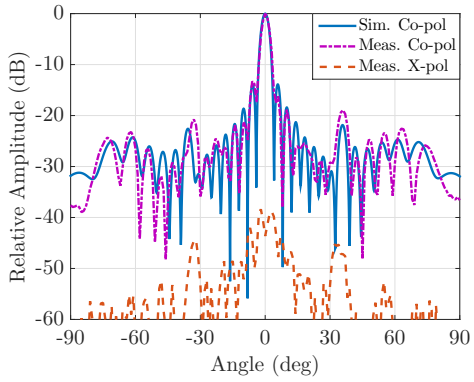

(a)

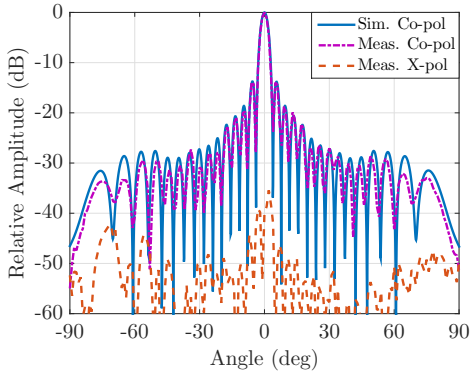

(b)

Fig. 7. Measured and Simulated radiation patterns of the integrated antenna-diplexer at 86 GHz. (a) E-plane, (b) H-plane.

TABLE I
SUMMARY OF THE MEASURED PERFORMANCE OF THE INTEGRATED RADIO FRONT-END

Parameter	71-76 GHz	81-86 GHz
Diplexer insertion loss (dB)	0.5	0.5
Antennas+diplexer gain (dBi)	31	31.5
Microstrip to GGW transition loss (dB)	0.31	0.31
Transmitter gain (dB)	24	21
Transmitter P_{1dB} (dBm)	14	16
Receiver gain (dB)	20	24

Fig. 8 shows the experimental setup used to transmit quadrature amplitude modulation (QAM) data by using an oscilloscope. The QAM modulated IQ signals at 2.5 GHz center IF frequency are produced by a Tektronix AWG7102 arbitrary waveform generator (AWG). A Pseudo-Random Binary Sequence (PRBS-9) pattern is mapped to gray-coded QAM modulated symbols. We have used a root-raised cosine (RRC) filter for pulse shaping with a roll-off factor of 0.35. The AWG's outputs are connected to the Tx IF ports of the integrated radio front-end module, where it up-converts and sends the data at E-band. The LO frequency is provided by an Agilent E8257D signal generator.

The other module receives and down-converts the RF signal to IF, where it is connected to a real-time Teledyne Lecroy oscilloscope with 100 GHz bandwidth. We have used the built-in Teledyne VSA software to demodulate and analyze the received data. A separate signal generator is used to provide LO for the RX module. The two modules are separated only 6 m due to the limited space in the lab measurements. The gain and output power of the Tx MMIC can be controlled by a Variable Gain Amplifier (VGA). Therefore, to avoid saturation of the receiver at the other side of the link, we have decreased the Tx output power as well as slightly misaligned the two antennas. The constellation and eye diagrams for 16-QAM and 32-QAM modulations with different data rates are also presented in Fig. 9.

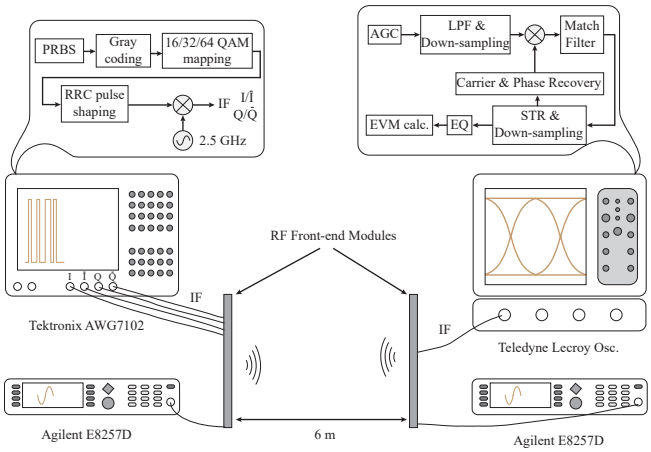

Fig. 8. Sketch of the data transmission test setup by using an oscilloscope.

TABLE II
SUMMARY OF LINK PERFORMANCE USING THE EXPERIMENT SETUP SHOWN IN FIG. 9

Center Freq. (GHz)	Modulation	Symbol/Data rate (GBaud/s)/(Gbit/s)	Spectral eff. (bit/s/Hz)	EVM* (%)
72.1	16	1/4	2.96	5.3
	32	1/5	3.7	5.9
	64	1/6	4.44	4.76
73	16	2/8	2.96	9.5
74.6	16	1/4	2.96	5.25
	32	1/5	3.7	5.8
	64	1/6	4.44	4.8
82.1	16	1/4	2.96	5.1
	32	1/5	3.7	5.65
	64	1/6	4.44	4.7
83	16	2/8	2.96	9.3
84.6	16	1/4	2.96	5.25
	32	1/5	3.7	5.6
	64	1/6	4.44	4.73

* Error Vector Magnitude

A summary of the achieved data rate and spectral efficiency for different modulation schemes is given in Table II. A maximum data rate of 8 Gbit/s is achieved by using 16-QAM modulation with spectral efficiency of 2.96 b/s/Hz. The spectral efficiency can be further improved by using higher order modulation. A data rate of 6 Gbit/s with spectral efficiency of 4.4 bit/s/Hz is obtained using 64-QAM modulated signal.

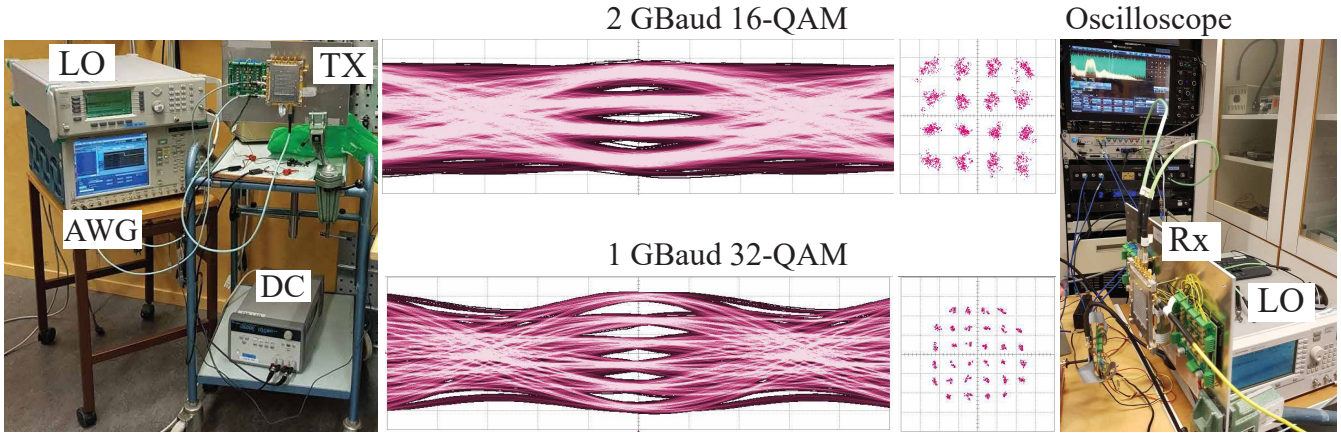

Fig. 9. Photograph of the experiment setup of Fig.8, and screen shots of 16 and 32-QAM received signal constellations.

IV. Conclusion

The realization and experimental validation of a compact integrated solution for multi-Gbit/s data transmission for point-to-point wireless link applications at E-band have been presented. The proposed module has a multi-layer architecture, where four unconnected layers are vertically stacked-up without the need for good electrical contact among them by using gap waveguide technology. A high gain slot array antenna, a diplexer, and millimeter-wave active circuitry are integrated in a compact geometry to design a full-duplex FDD radio front-end. The realized gap waveguide based radio front-end provides the advantages of low loss, high efficiency, compact integration, as well as assembly flexibility, which makes it a suitable solution for small cell backhaul links. The proposed integrated module shows the interesting mechanical flexibility and great potential that gap waveguide technology can offer in system integration including packaging with high complexity.

References

[1] D. Lockie and D. Peck, "High-data-rate millimeter-wave radios," *IEEE Microwave Magazine*, vol. 10, no. 5, 2009.

[2] X. Xu, M. Zhang, J. Hirokawa, and M. Ando, "E-band plate-laminated waveguide filters and their integration into a corporate-feed slot array antenna with diffusion bonding technology," *IEEE Transactions on Microwave Theory and Techniques*, vol. 64, no. 11, pp. 3592–3603, 2016.

[3] A. Vosoogh, M. S. Sorkherizi, A. U. Zaman, J. Yang, and A. A. Kishk, "An E-band antenna-diplexer compact integrated solution based on gap waveguide technology," in *Proceedings of the 2017 International Symposium on Antennas and Propagation (ISAP)*. Phuket, 2017, pp. 1–2.

[4] P.-S. Kildal, "Artificially soft and hard surfaces in electromagnetics," *IEEE Transactions on Antennas and Propagation*, vol. 38, no. 10, pp. 1537–1544, 1990.

[5] P.-S. Kildal, E. Alfonso, A. Valero-Nogueira, and E. Rajo-Iglesias, "Local metamaterial-based waveguides in gaps between parallel metal plates," *IEEE Antennas and Wireless Propagation Letters*, vol. 8, pp. 84–87, 2009.

[6] E. Rajo-Iglesias and P.-S. Kildal, "Numerical studies of bandwidth of parallel-plate cut-off realised by a bed of nails, corrugations and mushroom-type electromagnetic bandgap for use in gap waveguides," *IET Microwaves, Antennas and Propagation*, vol. 5, no. 3, pp. 282–289, 2011.

[7] A. Vosoogh and P.-S. Kildal, "Corporate-fed planar 60 GHz slot array made of three unconnected metal layers using AMC pin surface for the gap waveguide," *IEEE Antennas and Wireless Propagation Letters*, vol. 15, pp. 1935–1938, Dec. 2015.

[8] P. Taghikhani, J. Yang, and A. Vosoogh, "High gain V-band planar array antenna using half-height pin gap waveguide," in *Proceedings of the 11th European Conference on Antennas and Propagation (EuCAP)*. Paris, 2017, pp. 2758–2761.

[9] A. Vosoogh, P.-S. Kildal, V. Vassilev, A. U. Zaman, and S. Carlsson, "E-band 3-D metal printed wideband planar horn array antenna," in *Proceedings of the 2016 International Symposium on Antennas and Propagation (ISAP)*. Okinawa, Japan, 2016.

[10] J. Liu, A. Vosoogh, A. U. Zaman, and J. Yang, "Design and fabrication of a high-gain 60-GHz cavity-backed slot antenna array fed by inverted microstrip gap waveguide," *IEEE Transactions on Antennas and Propagation*, vol. 65, no. 4, pp. 2117–2122, 2017.

[11] A. Vosoogh, P.-S. Kildal, and V. Vassilev, "Wideband and high-gain corporate-fed gap waveguide slot array antenna with ETSI class II radiation pattern in V-band," *IEEE Transactions on Antennas and Propagation*, 2016.

[12] D. Zarifi, A. Farahbakhsh, and A. U. Zaman, "A gap waveguide-fed wideband patch antenna array for 60-GHz applications," *IEEE Transactions on Antennas and Propagation*, vol. 65, no. 9, pp. 4875–4879, 2017.

[13] [online] Available: *http://www.gotmic.se/txrx.html*, Sep. 2018.